Supporting Information

Covalent Grafting of P-phenylenediamine Molecule onto "Bubble-like" Carbon Surface for High Performance Asymmetric Supercapacitors

Chao Huangfu,‡[ab] Zheng Liu,‡*[a] Qihang Zhou,[b] Lin Wang,[a] Tong Wei,[ab] Zhipeng Qiu,[a] Su Zhang,[c] Zhuangjun Fan*[ab]

a. School of Material Science and Engineering, China University of Petroleum, Qingdao 266580, China

b. Key Laboratory of Superlight Materials and Surface Technology, Ministry of Education, College of Material Science and Chemical Engineering, Harbin Engineering University, Harbin 150001, China

c. Key Laboratory of Energy Materials Chemistry, Ministry of Education; Key Laboratory of Advanced Functional Materials, Autonomous Region; Institute of Applied Chemistry, Xinjiang University, Urumqi, 830046, P. R. China. E-mail: liuzhengbeyond@163.com; fanzhj666@163.com

‡ These authors contributed equally to this work.

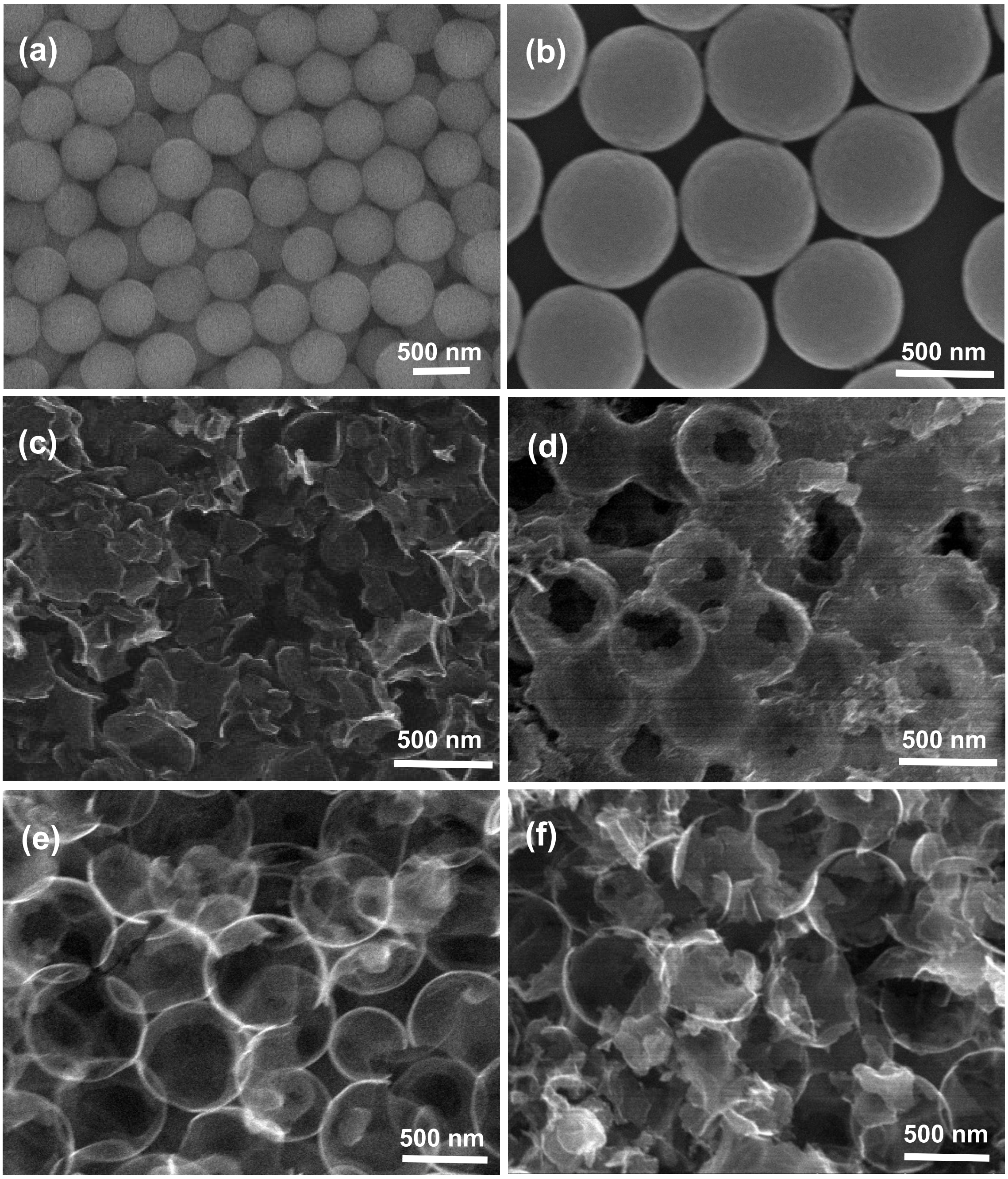

Fig. S1. SEM images of the (a, b) SiO_2, (c) BC-0, (d) BC-0.25, (e) BC-0.5, (f) BC-1.

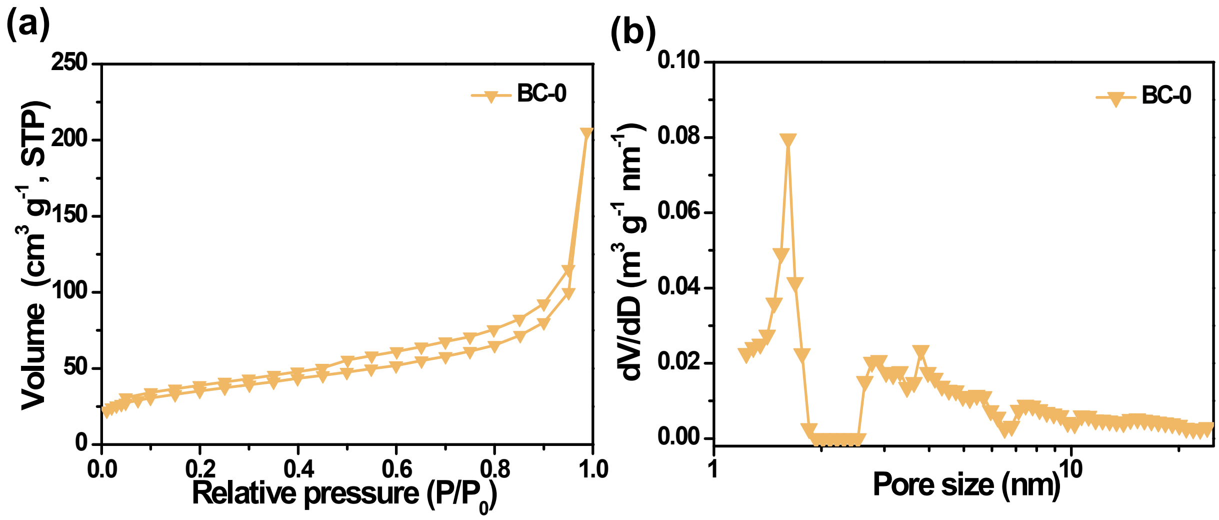

Fig. S2. (a, b) Nitrogen adsorption-desorption isotherms and relative pore size distributions of BC-0.

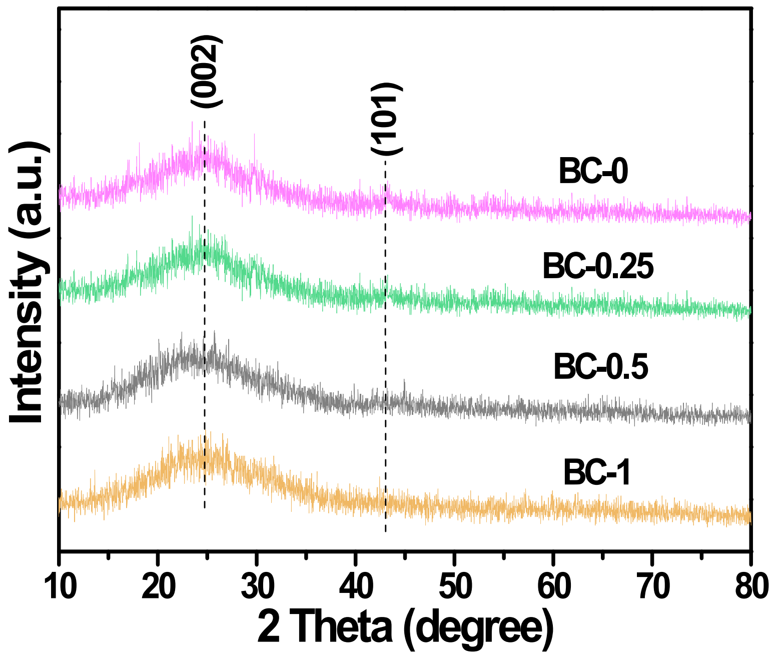

Fig. S3. XRD patterns of BC-x (x=0, 0.25, 0.5, 1).

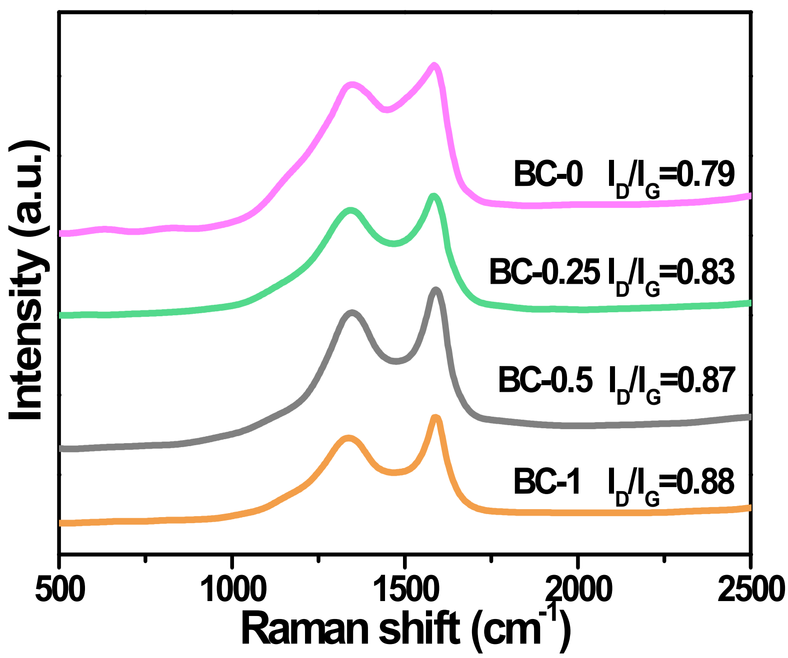

Fig. S4. Raman spectra of BC-x (x=0, 0.25, 0.5, 1).

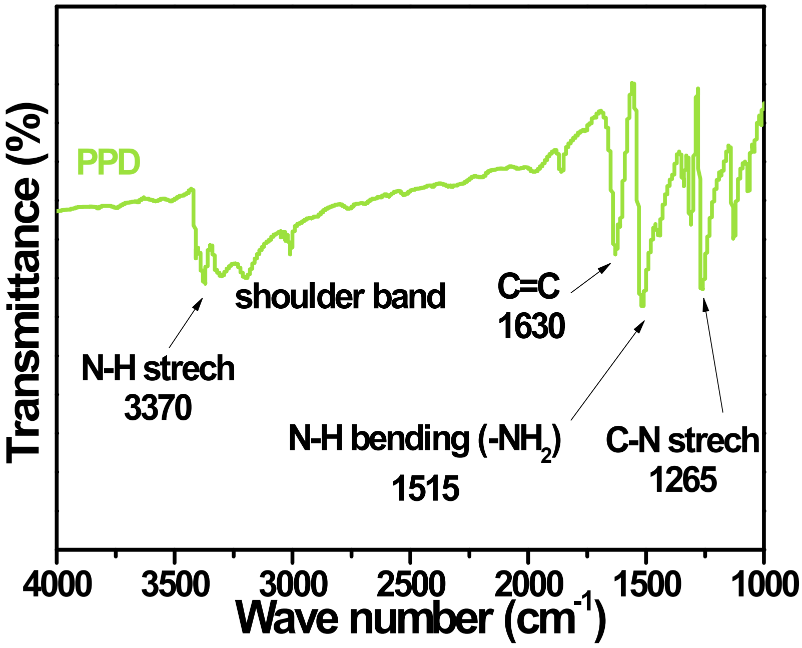

Fig. S5. FTIR spectra of PPD.

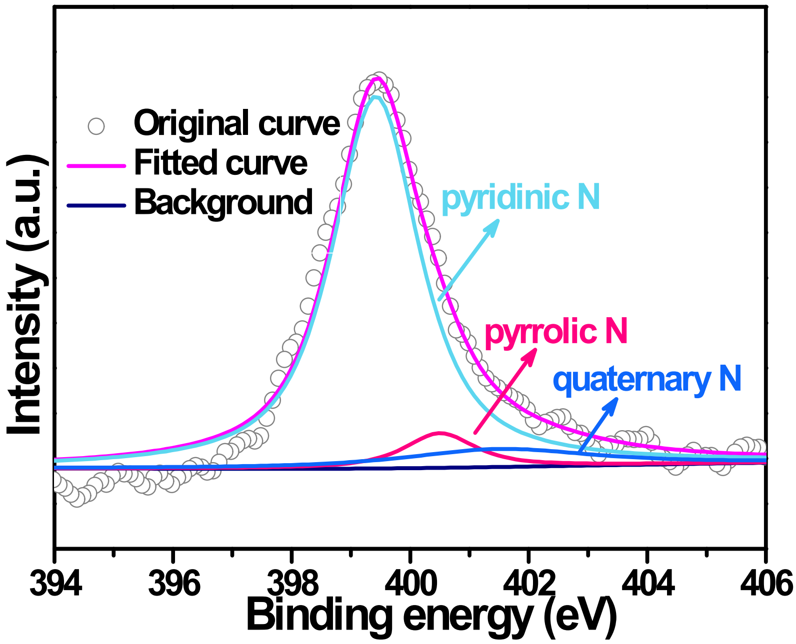

Fig. S6. High-resolution N 1s spectra of the PPD-BC.

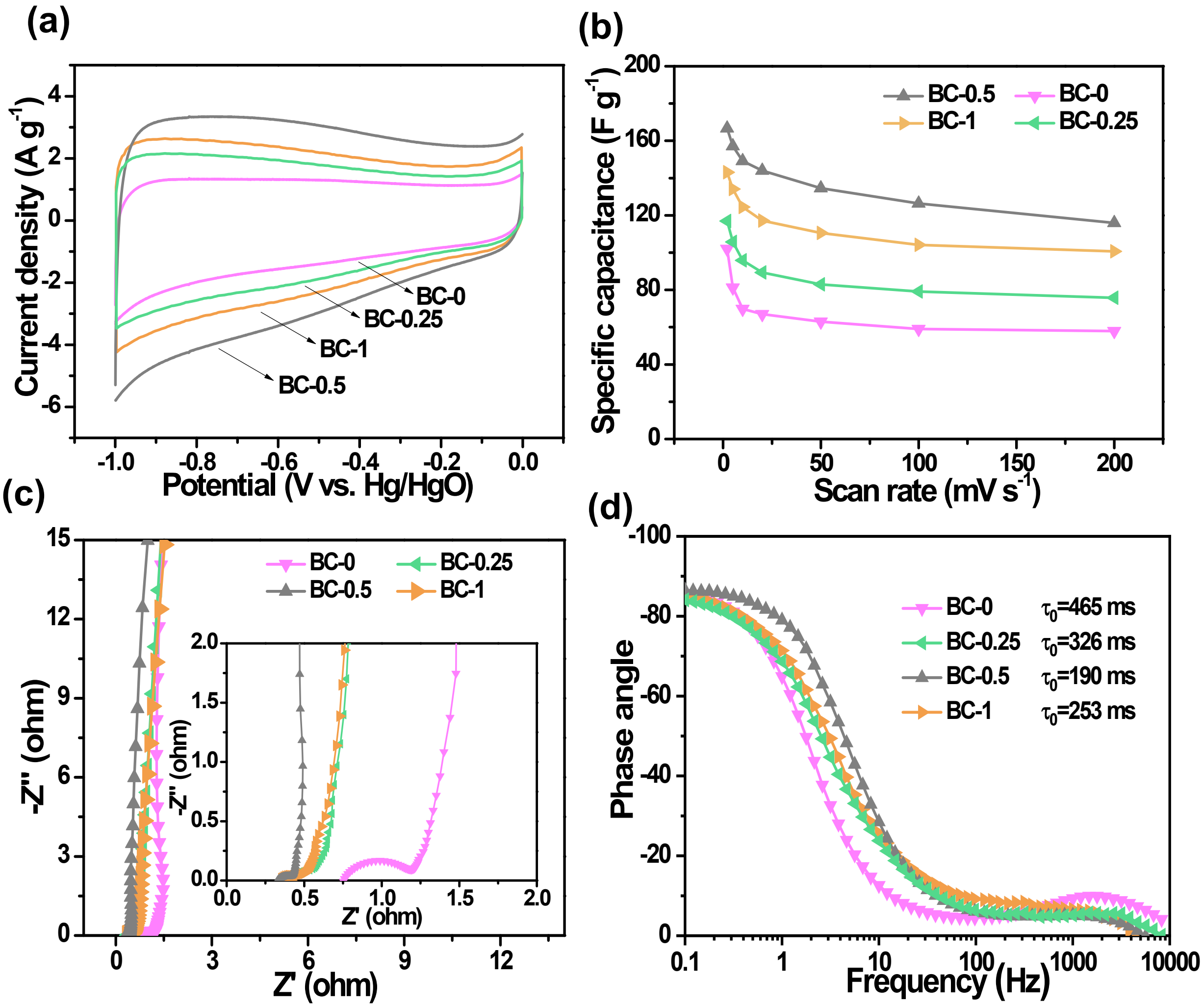

Fig. S7. Electrochemical performance of BC-x (x=0, 0.25, 0.5, 1). (a) CV curves at 20 mV s^{-1}. (b) Specific capacitance as a function of scan rate. (c) Nyquist plots. (d) Bode plots

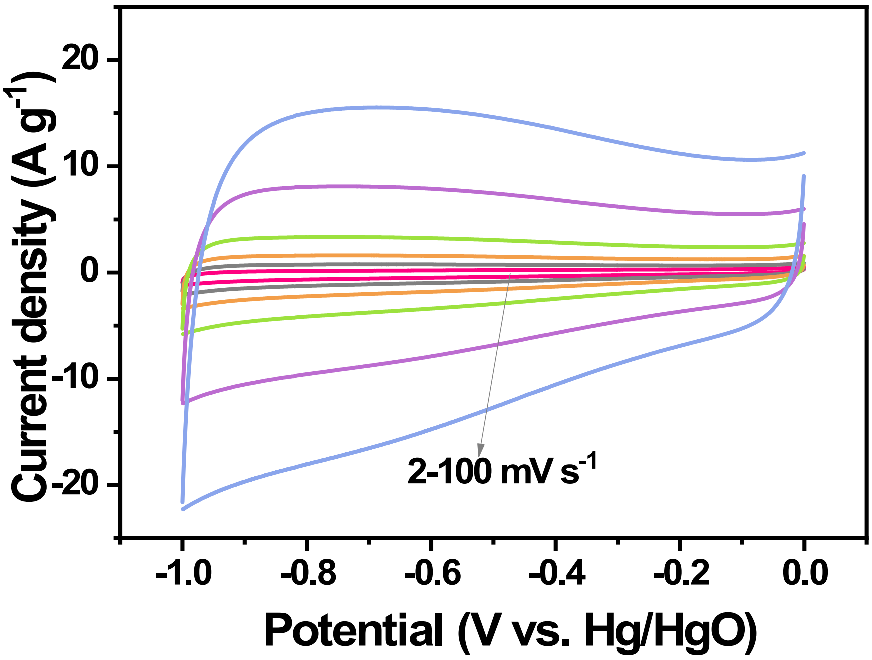

Fig. S8. CV curves of the BC-0.5 at the scan rates from 2 to 100 mV s^{-1}

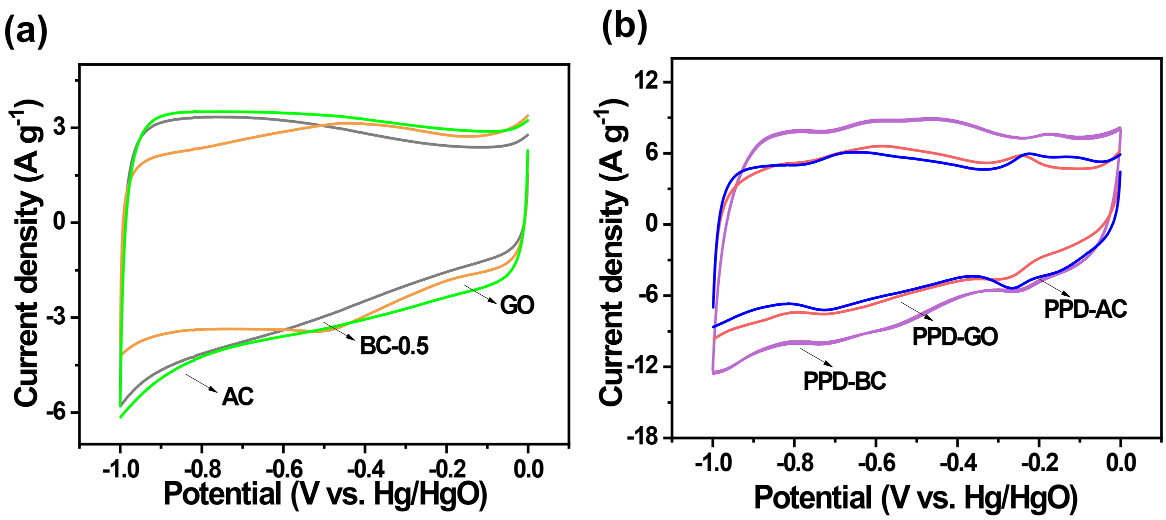

Fig. S9. (a) CV curves of the AC, GO, and BC-0.5 at 20 mV s^{-1} (b) CV curves of the PPD-AC, PPD-GO, and PPD-BC at 20 mV s^{-1}.

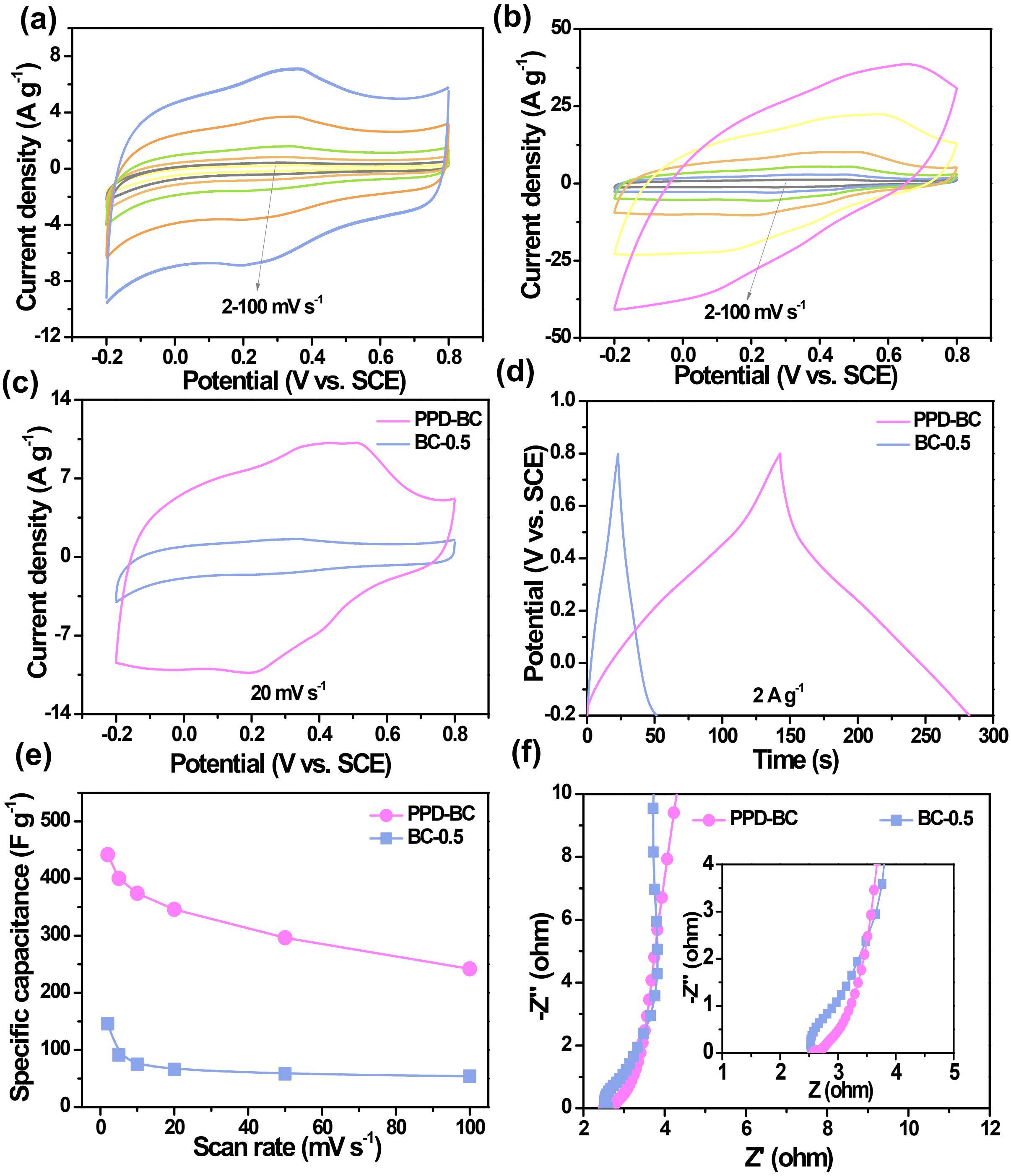

Fig. S10. The electrochemical performances of the BC-0.5 and PPD-BC using a three-electrode cell in 1 M H_2SO_4 electrolyte within a potential window of -0.2 to 0.8 V (vs. SCE)**.** CV curves of the (a) BC-0.5 and (b) PPD-BC at different scan rates. (c) CV curves of the BC-0.5 and PPD-BC at 20 mV s^{-1}. (d) Galvanostatic charge/discharge curves of the BC-0.5 and PPD-BC at 2 A g^{-1}. (e) Specific capacitances of the BC-0.5 and PPD-BC at different scan rates from 2 to 100 mV s^{-1}. (f) Nyquist plots with inset showing the zoom-in views of the high-frequency region.

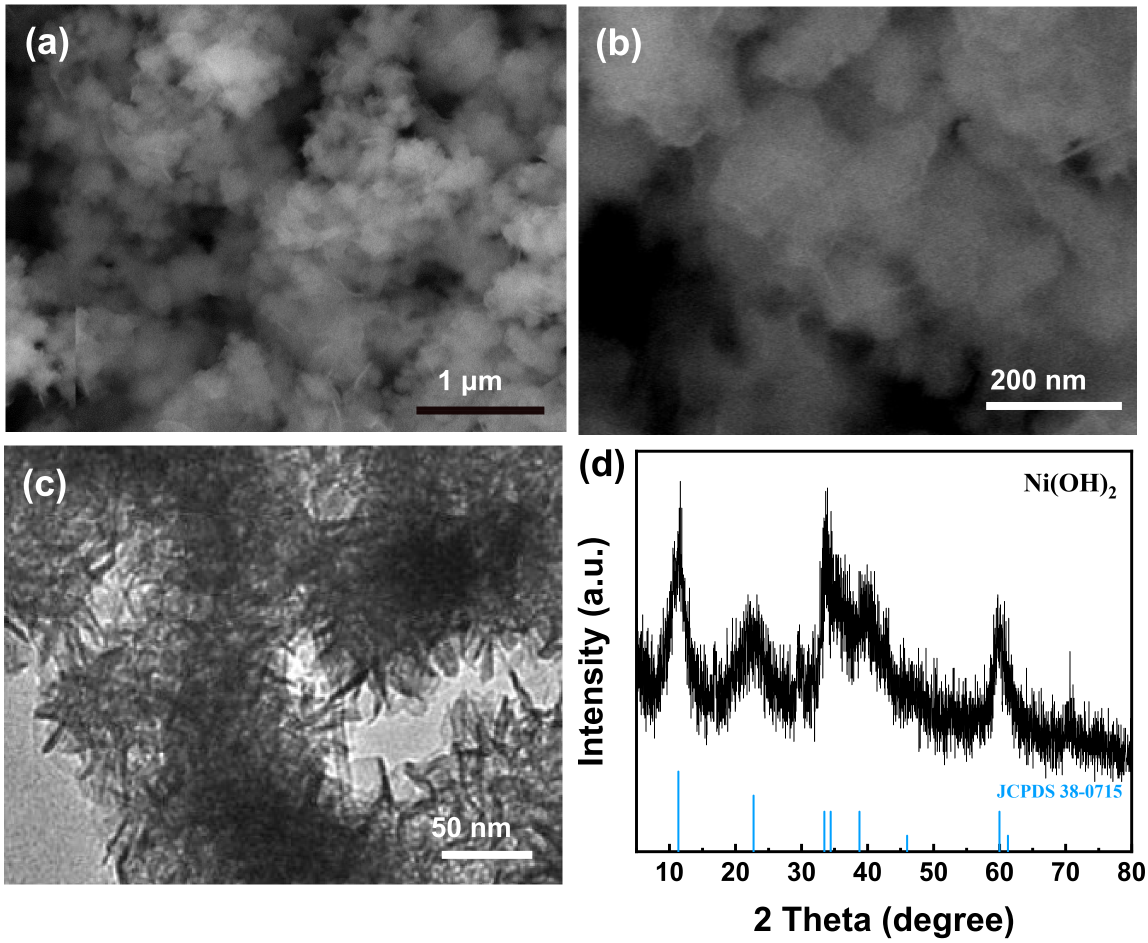

Fig. S11. (a, b) SEM and TEM images of the $Ni(OH)_2$. (d) XRD patterns of $Ni(OH)_2$.

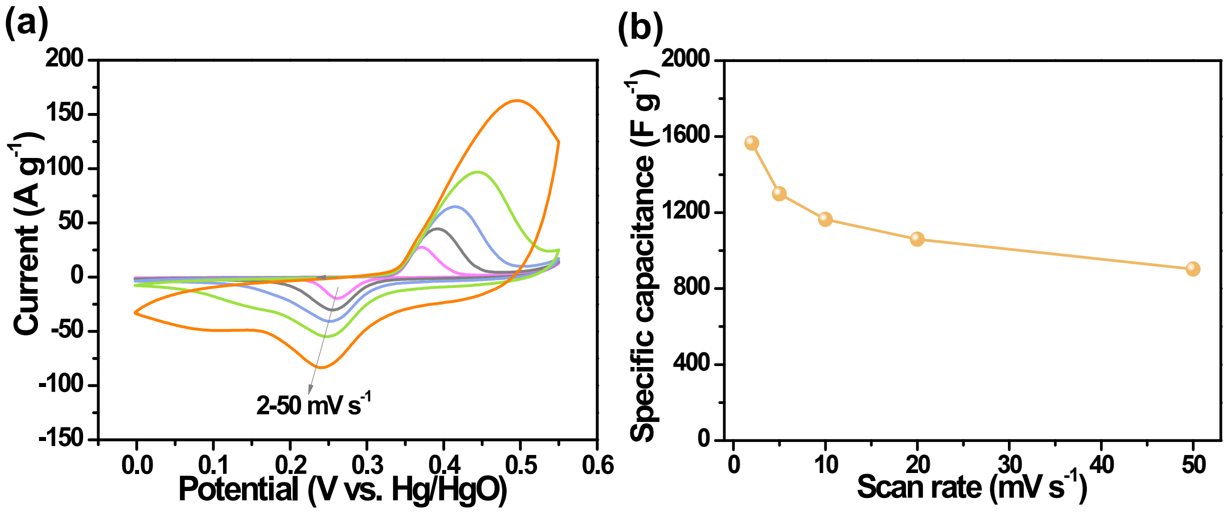

Fig. S12. Electrochemical performance of $Ni(OH)_2$. (a) CV curves at different scan rates from 2 to 50 mV s^{-1}. (b) Specific capacitance at different scan rates from 2 to 50 mV s^{-1}.

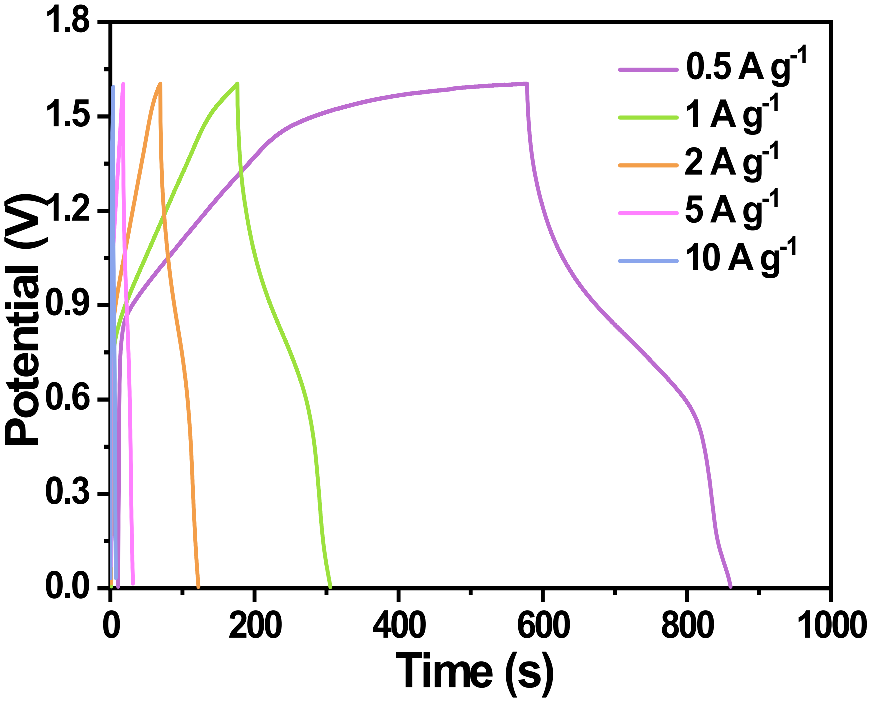

Fig. S13. Galvanostatic charge/discharge curves of the PPD-BC//$Ni(OH)_2$ ASC at various current densities from 0.5 to 10 A g^{-1}.

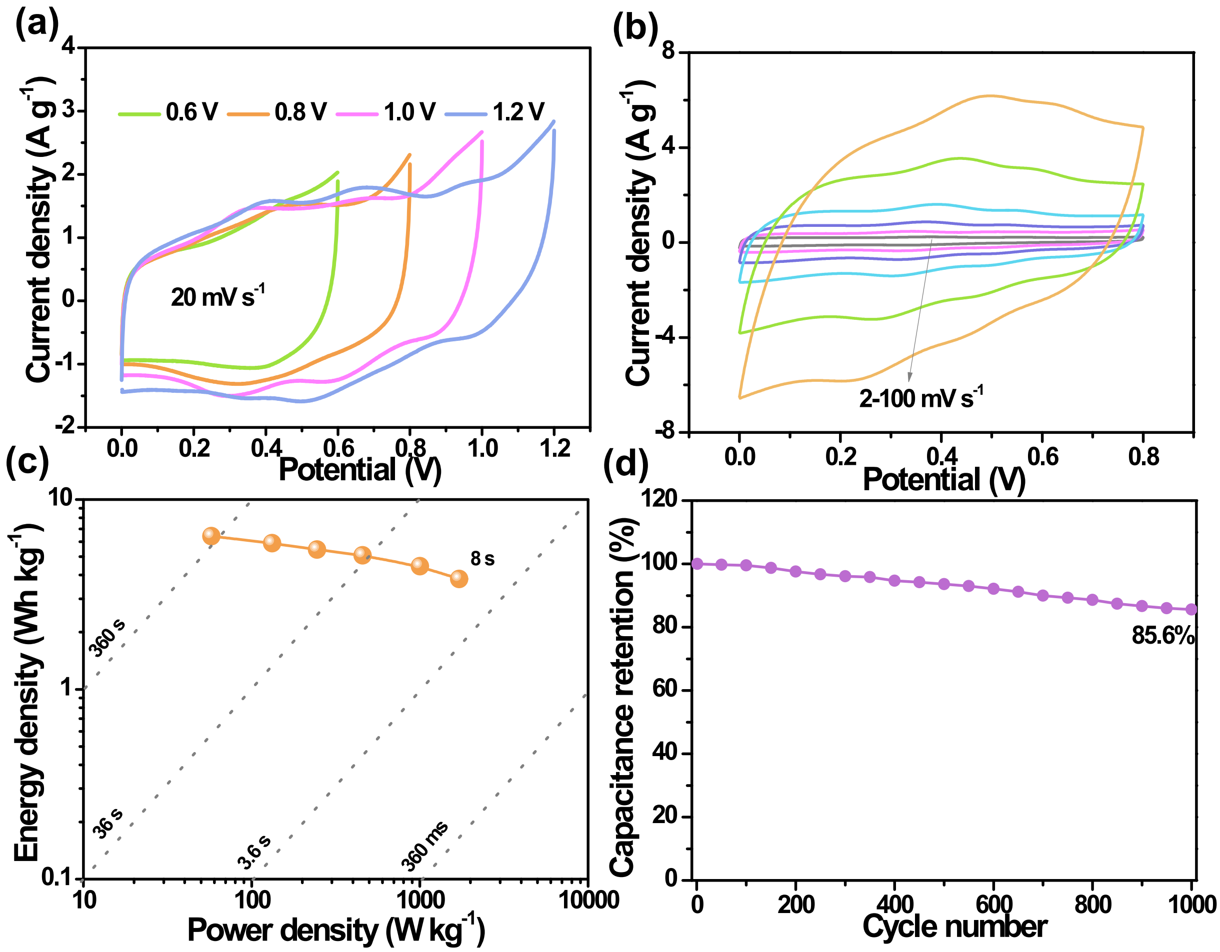

Fig. S14. Electrochemical performance of the PPD-BC//PPD-BC symmetric supercapacitor in 1 M H_2SO_4 electrolyte. (a) CV curves in various operating voltage. (b) CV curves at different scan rates. (c) Ragone plots. (d) Cycling stability at 50 mV s^{-1}.

Table S1. Comparison of the performances for previously reported ASCs.

Electrode materials		Voltage (V)	Electrolyte	Energy density (Wh kg^{-1})	Power density (W kg^{-1})	Ref
Positive electrode	**Negative elecrode**					
hexagonal boron nitride	AC	1.45	2 M KOH	17	245	47
$NiCo_2O_4$	AC	1.4	2 M KOH	24.5	175	45
MnOOH/NiAl-LDH	AC	1.6	6 M KOH	26.8	800	46
PPFPC-NiO	AC	1.5	6 M KOH	32.2	281.3	49
$NiCo_2O_4$	nitrogen-doped porous carbon	1.4	2 M KOH	32	700.4	48
HPC-2/MnO_2	honeycomb porous carbon	2	1 M Na_2SO_4	58.8	210.7	50
$Ni(OH)_2$	PPD-BC	1.6	2 M KOH	94	423	This work